OPEN ACCESS
ARTICLE

Direct Synthesis of α-Silicon Nitride Nanowires from Silicon Monoxide on Alumina

Regular Paper

Jiang Cui[1], Bin Li[1]*, Chunrong Zou[1], Changrui Zhang[1] and Siqing Wang[1]

1 Science and Technology on Advanced Ceramic Fibers and Composites Laboratory, College of Aerospace Science and Engineering, National University of Defense Technology, Changsha, Hunan Province, China
*Corresponding author(s) E-mail: libin@nudt.edu.cn

Received 23 June 2015; Accepted 01 October 2015

DOI: 10.5772/61661

Abstract

Silicon nitride nanowires were synthesized using silicon monoxide as raw materials and an alumina plate as substrate at 1500°C. The obtained nanowires were characterized by X-ray diffraction, Fourier transform infrared spectroscopy, scanning electron microscopy, high-resolution transmission electron microscopy and thermogravimetric-differential scanning calorimetry. The results revealed that silicon nitride nanowires possess a diameter of about 200 nm and a length of several hundred micrometres. The preferred growth direction of the nanowires was [100]. The chemical and structural composition of the silicon nitride nanowires were also studied and were shown to have a composition of primarily α-Si_3N_4. The temperature for fierce oxidation in air was above 1135°C. The formation mechanism of silicon nitride nanowires was assumed to be a vapour-solid (VS) process.

Keywords Silicon Nitride Nanowires, Nitridation, Silicon Monoxide, Alumina

1. Introduction

One dimensional nanoscale materials always have a range of excellent properties due to their special structure and limited dimensions. As one type of one dimensional nanoscale materials, silicon nitride (Si_3N_4) nanowires possess a series of unique properties, such as high fracture toughness, high elastic modulus, light weight and good resistance to thermal shock and oxidation [1-2]. Consequently, Si_3N_4 nanowires show great potential as reinforcement materials, especially at high temperatures. Additionally, Si_3N_4 ceramic demonstrates a relatively low dielectric constant, 5.6 for α-Si_3N_4 and 7.9 for β-Si_3N_4, respectively. For α-Si_3N_4 nanowires, the dielectric constant is slightly elevated due to the small size effect [3]. Nevertheless, α-Si_3N_4 nanowires remain a promising material in wave-transparent devices, especially for window antennae and high speed radomes [4]. In addition, Si_3N_4 serves as a wide band-gap semiconductor with excellent chemical stability and creep resistance. In nanoscale dimensions, many novel properties such as photoluminescence, caused by the basic effects of nanomaterials, will be prevalent. Thus, Si_3N_4 nanowires hold potential for application in electronic and optic nanodevices [5].

In recent years, the synthesis of Si_3N_4 nanowires has gained significant attention. Many different methods are used to synthesize Si_3N_4 nanowires, including carbothermic reduction [6-8], oxide-assisted growth [9], chemical vapour deposition [10], nitridation of silicon powders [11-15], combustion synthesis [16], solvothermal synthesis [17], etc.

Among all these preparation methods, those with vapour phase acting as the media phase stand out as the most common route in the synthesis of high-quality nanowires, although other growth techniques, especially solution phase models, also offer unique advantages [18]. For vapour phase methods, various types of raw materials are used such as Si powders, SiO_2 powders, as well as sol-gel or blending carbon with these materials. However, some reports have attempted to use a mixture of active carbon and SiO as raw materials to synthesize Si_3N_4 nanowires [19]; furthermore, reports have on rare occasions used single SiO as a silicon source for synthesizing Si_3N_4 nanowires [20]. In this paper, we used only SiO as a silicon source to synthesize Si_3N_4 nanowires on an alumina (Al_2O_3) plate; special attention was given to the controlling of the reaction's atmosphere density. The resistance of the nanowires to oxidation at high temperatures and surface states were also evaluated and the formation process and mechanism of the nanowires were discussed.

2. Experimental Procedure

The silicon source used in this study was SiO particles (99.99%, Xiya Reagent), which was source ground over several hours into a powder. An Al_2O_3 plate (50.0 mm × 50.0 mm ×2.0 mm) was used as the substrate for the growth of Si_3N_4 nanowires. The plate was polished and ultrasonically washed in ethanol for 40 minutes, then dried overnight at 80°C in a drying oven. Then, the silicon source powders were placed in a cylindrical graphite crucible, and the Al_2O_3 plate was covered upon the cylindrical crucible. The cylindrical graphite crucible was then placed at the centre of a graphite furnace. After replacing the air with high purity N_2 (purity 99.999%), the furnace was heated to 1500°C over three hours and kept at this temperature for two hours, then cooled down to room temperature at a rate of 5°C per minute. The N_2 was maintained at a rate of 400 sccm (standard cubic centimetres per minute) during the entire heating and cooling procedure.

The wool-like products were collected on the surface of the Al_2O_3 plate. The obtained products were characterized by Field emission scanning electron microscopy (SEM, S4800; Hitachi, Japan & Quanta-200; FEI, Holland), X-ray diffraction (XRD, TTR-3; Rigaku, Tokyo, Japan) with CuK_α radiation, Fourier transform infrared spectra (FTIR, Avatar 360, Nicolet, Madison, WI), high-resolution transmission electron microscopy (HRTEM, FEI Tecnai G2F20), X-ray photoelectron spectroscopy (XPS, ESCALAB 250Xi) and thermogravimetric-differential scanning calorimetry (TG-DSC, NETZSCH STA 449F3).

3. Results and Discussion

The XRD patterns of the obtained products and commercial α-Si_3N_4 powders are shown in Figure 1a. The results revealed that the synthesized nanowires were mainly α phase Si_3N_4 (PDF No.09-0250), accompanied by a small amount of β phase Si_3N_4 (PDF No.33-1160). The composition of the products appears to be extremely similar to commercial α-Si_3N_4 powders. This contributes to an explanation for why the synthesis temperature of β-Si_3N_4 is higher than α-Si_3N_4 and why α-Si_3N_4 seldom transforms to β-Si_3N_4 in the experiment environment described above. X-ray diffractions were also completed for the residual materials following the reaction. Three new phases (Si, Si_2N_2O, SiC) were generated from the raw materials and this can be connected to the mechanism for the entire reaction. An additional test was then conducted by FTIR. Figure 2 shows the infrared absorbance spectra for the mixture of the milled Si_3N_4 nanowires and KBr. The strongest peak at 844 cm^{-1} and the following peak at 884 cm^{-1} are related to different Si-N stretching modes; then, the peak at 680 cm^{-1} may correspond to a Si-Si stretching mode [21]. These results further verify the composition of the nanowires. The peak at 1041 cm^{-1} is associated with a Si-O-Si stretching mode [22] and reveals that the Si_3N_4 nanowires possess oxygen, and bonds with silicon.

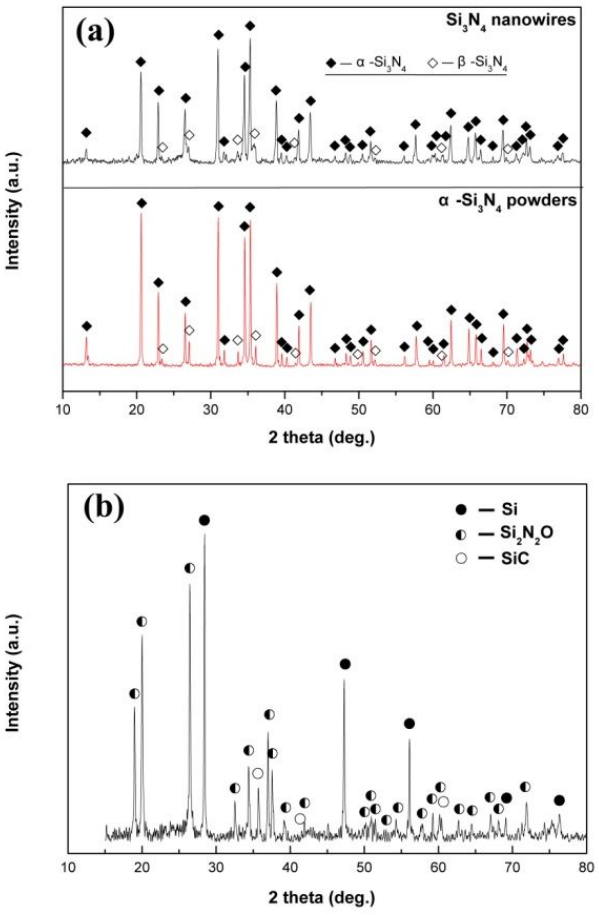

Figure 1. (a) XRD patterns of the as-received Si_3N_4 nanowires and commercial α-Si_3N_4 powders; (b) XRD pattern of residual materials after reaction

The microcosmic morphologies of the Si_3N_4 nanowires were observed by SEM. Figures 3 (a-b) show that the obtained nanowires possessed a cylindrical structure with a smooth surface and a diameter of nearly 80~250 nm. As Figure 3c shows, most of the nanowires grew to a diameter

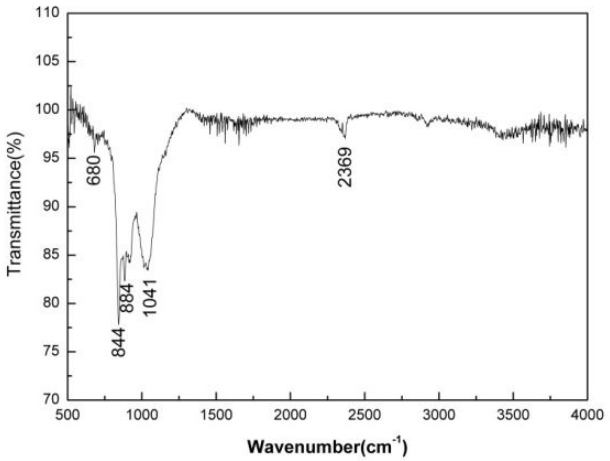

Figure 2. FTIR spectrum of Si_3N_4 nanowires synthesized by nitridation of SiO at 1500°C

of about 200 nm, while there were several bold nanowires with a diameter of 500 nm. No droplets were found on the tip of the nanowires. Figure 3d shows that large quantities of aligned nanowires grew homogeneous on the surface of the Al_2O_3 plate and attained a length of several hundred micrometres. The bending morphologies of several nanowires also suggest a superior flexural strength.

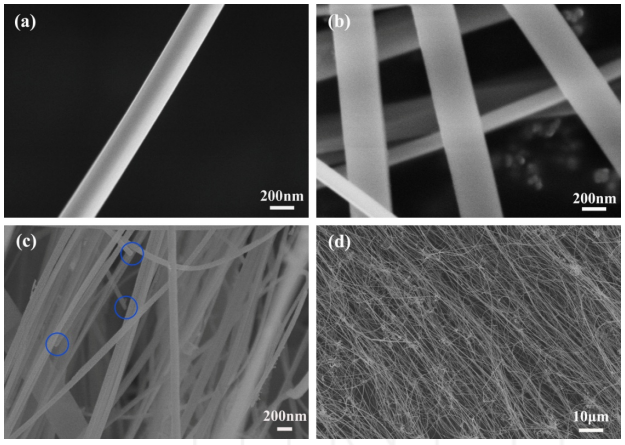

Figure 3. (a) SEM of single Si_3N_4 nanowires with smooth surface; (b) SEM of Si_3N_4 nanowires with a diameter of nearly 80~250 nm; (c) SEM of several Si_3N_4 nanowires without droplets; (d) SEM of aligned Si_3N_4 nanowires grown on the alumina substrate

Further characterization of the synthesized nanowires was completed using HRTEM. As Figure 4a shows, the nanowires possessed a diameter of 80 nm and 190 nm. The fragments scattering around the nanowires were caused by the grinding of products during sample preparation. The crystal structure is given by Figure 4b. The spacing distances between two adjacent fringes in different planes had an equal value of 0.672 nm, which was consistent with the distance of [100] planes of the hexagonal crystal lattice of α-Si_3N_4 with a space group of P31c(159). The spacing between lattice planes, as well as atom distribution also indicated a preferred growth direction of [100,23-24]. The surfaces of the nanowires were sometimes coated with thin amorphous layers. This can often be observed in many synthesized Si_3N_4 nanowires [25].

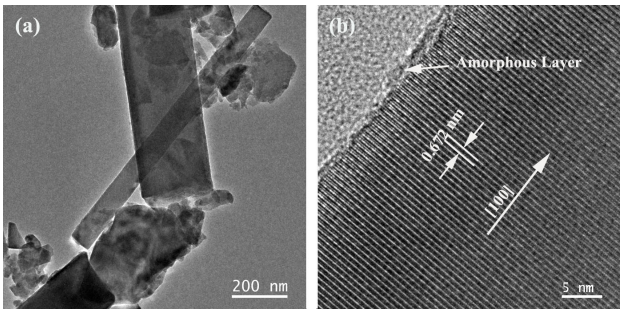

Figure 4. (a) TEM image of the α-Si_3N_4 nanowires surrounded by scattered fragments; (b) TEM and FFT image of the α-Si_3N_4 nanowires with a spacing distance of 0.672 nm and a growth direction of [100], corresponding to hexagonal α-Si_3N_4

To further investigate the surface states of the Si_3N_4 nanowires, depth profile by XPS was conducted with different etch times; element messages with different depths are also shown in Figure 1 and Table 1. The results revealed that the surface of the Si_3N_4 nanowires contained a Si element, N element, O element and a C element. The C element and part of the O element were derived from common contamination impurities inherent in XPS tests. Regardless of this, the variation trend among elements could still be observed via the XPS spectrum of the typical Si_3N_4 nanowires. With an increase in etch level, the content of the Si element and N element increased correspondingly. Meanwhile, the content of the C element and O element sharply decreased. This result notes the gradual change of elements in the amorphous layers of the Si_3N_4 nanowires, as shown in the TEM image.

The XPS spectrum of the Si element was also investigated. The peak positions of Si2p were found to be in the surface shift between 101.78 eV and 102.48 eV. The binding energy scale of Si2p in monatomic Si is 97.7-99.2 eV. Here, we can infer that there was no monatomic Si in the surface of Si_3N_4 nanowires, because there was no peak position lower than 100 eV. The O element, except for the impurity in the test, was primarily derived from SiO_x (peak position at Si2p: 102 eV). Meanwhile, the peak position of the O element in SiOx also corresponded to Table 1, which can be assumed as evidence for the existence of SiOx. The O element in the surface of nanowires may have been derived from the impurity of the N_2 and the growth process.

Sample	Etch Level / nm	Mole percent of atom /At%			Peak position /eV		
		Si2p	N1s	O1s	Si2p	N1s	O1s
1	0	43.61	38.46	17.93	102.12	397.75	532.14
2	1	47.78	39.15	13.07	101.91	397.6	532.21
3	2	48.57	39.43	11.99	101.9	397.63	532.24

Table 1. Mole per cent and peak position of Si, N and O at different etch levels

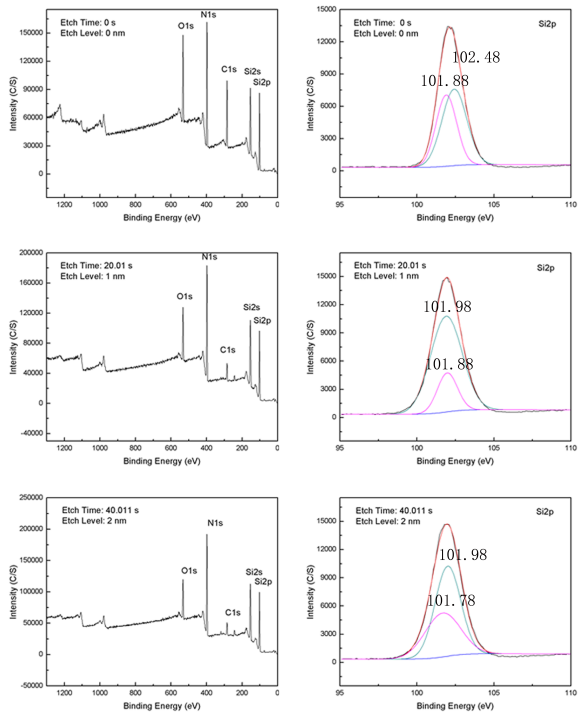

Figure 5. XPS spectrum of the typical Si_3N_4 nanowires and Si element

The resistance of the Si_3N_4 nanowires to oxidation at high temperatures was evaluated by TG-DSC in air. As Figure 5 shows, the weight of the nanowires remained steady at a relatively low temperature and rose sharply when at temperatures above 1135 °C. Two exothermic peaks emerged in the position of 1210°C and 1290°C. This may correlate with the two reactions presented below:

$$2Si_3N_4(s) + 1.5O_2(g) \rightarrow 3Si_2N_2O(s) + N_2(g) \quad (1)$$

$$Si_3N_4(s) + 3O_2(g) \rightarrow 3SiO_2(s) + 2N_2(g) \quad (2)$$

Compared to the bulk of Si_3N_4 materials, Si_3N_4 nanowires showed poor performance regarding oxidation resistance. The oxidation resistance ability of Si_3N_4 ceramics ultimately rests on the integrity and stability of the surface oxide layer [26]. Considering their special morphology and limited diameter, the Si_3N_4 nanowires find it difficult to form an integrated surface oxide layer prior to absolute oxidation. Their limited diameter also leads to forming a large specific surface area and high surface energy. Hence, Si_3N_4 nanowires react with oxide more easily than bulk Si_3N_4.

For the growth process, vapour phase growth was extensively used for producing nanowires; additionally, several models, including vapour-solid (VS) and vapour-liquid-solid (VLS) mechanisms were proposed to explain the growth mechanism for crystalline nanowires [27]. Compared to the VS mechanism, the VLS mechanism possesses

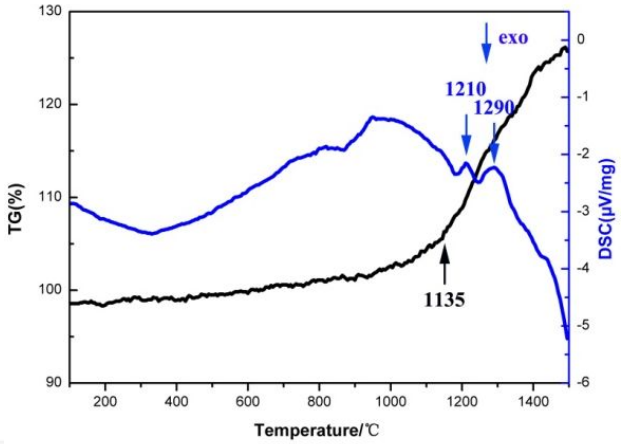

Figure 6. TG-DSC data of Si_3N_4 nanowires in air at temperatures ranging from 100°C to 1500°C.

three growth stages: metal alloying, crystal nucleation and axial growth [28], resulting in the catalyst ball on the end of nanowire as a special morphological feature. Considering that no droplets were found on the end of nanowires and no metal catalyst was added, we prefer the VS mechanism for the growth process. This process includes three steps: evaporation, gaseous reaction and nucleation. With a rise in temperature, the SiO thermally decomposes to Si and SiO_2, and can be shown as follows:

$$2SiO(s) \rightarrow Si(g) + SiO_2(s) \quad (3)$$

The Si phase in the residual materials can also be formed in this way. As for the Si_2N_2O and SiC, these can be formed by the reaction of Si and SiO_2 with N_2 and the carbon on the graphite crucible with high activity.

Then, the vapour phase of Si reacts with N_2 as follow:

$$3Si(g) + 2N_2(g) \rightarrow Si_3N_4(s) \quad (4)$$

The newly generated Si_3N_4 then condenses and acts as the source for the original nucleus. Large quantities of nuclei are formed on the surface of the Al_2O_3 plate and lead to a high yield of nanowires. With the consistent transport of the vapour phase of Si to the surface of the nucleuses, the crystal Si_3N_4 grows as an epitaxial in the direction of the lowest energy found in crystallography, which was found to be [100]. Finally, the Si_3N_4 nanowires continue to grow via this typical VS process.

Since the vapour phase of Si is directly generated from the decomposition of raw materials, the density of the vapour phase can be high and as a result lead to inhomogeneous nanowires. For this research, we diluted the Si vapour by means of flowing N_2 and placed the Al_2O_3 plate in a position away from the raw materials. The results show that the nanowires grew homogeneously on the Al_2O_3 plate.

Meanwhile, a high flow rate of N_2 will reduce the growth of nanowires [29]. Hence, it is important to control the flow rate of the N_2.

4. Conclusions

In summary, Si_3N_4 nanowires were successfully synthesized using an Al_2O_3 plate as substrate and SiO as silicon source. Nanowires with an average diameter of 200 nm consisted primarily of α-Si_3N_4 and grew in the direction of [100] to a length of several hundred micrometres. Si_3N_4 nanowires will be significantly oxidized in air at a temperature above 1135°C. The growth process of the nanowires was inferred to be a VS mechanism. The proper flow rate is also essential for the yield and quality of nanowires. Considering the easy procedures and high yield, this method can be a good choice for the high yield of Si_3N_4 nanowires. The evaluation of oxidation resistance ability and the element message of the surface of the nanowires may also offer references to the application of Si_3N_4 nanowires.

5. Acknowledgements

The financial support of the National Science Foundation of China (No. 50902150), Aid Program for Science and Technology Innovation Research Team in Higher Educational Institution of Hunan Province, Aid Program for Innovative Group of National University of Defense Technology are all gratefully acknowledged.

6. References

[1] Zhang Y, Wang N, He R, Zhang Q, Zhu J, Yan Y (2000) Reversible bending of Si_3N_4 nanowire. Journal of Materials Research 15(05):1048-1051.

[2] Chen I W, Rosenflanz A (1997) A tough SiAlON ceramic based on α-Si_3N_4 with a whisker-like microstructure. Nature 389(6652):701-704.

[3] Xie T, Wu Y C, Cai W P, Zhang L D (2005) High purity alpha silicon nitride nanowires-synthesis and dielectric properties. Physica Status Solidi (A) Applications and Materials 202(10):1919 - 1924.

[4] Zou C R, Zhang C R, Li B, Wang S Q, Cao F (2013) Microstructure and properties of porous silicon nitride ceramics prepared by gel-casting and gas pressure sintering. Materials and Design 44:114-118.

[5] Deshmukh S, Jen K P, Santhanam S (2012) Comparison of silicon nitride nanofibers synthesized using silica nanopowders and silica gel. Materials Sciences and Applications 3(8):523-529.

[6] Li G Y, Li X, Wang H, Li Z Q (2008) Long silicon nitride nanowires synthesized in a simple route. Applied Physics A 93(2):471-475.

[7] Wu X C, Song W H, Zhao B, Huang W D, Pu M H, Sun Y P (2000) Synthesis of coaxial nanowires of silicon nitride sheathed with silicon and silicon oxide. Solid State Communications 115(12):683-686.

[8] Chaudhuri M G, Ahmadullah S, Dey R, Das G C, Mukherjee S, Mitra M K (2001) Novel technique for synthesis of silicon nitride nanowires. Advances in Applied Ceramics 110(4):211-214.

[9] Wang J, Li X L, Jin Z G, Ji H M (2014) Non-catalytic vapor synthesis of millimeter-scale α-Si_3N_4 nanowires from oxidized silicon powders. Materials Letters 124:249-252.

[10] Farjas J, Rath C, Pinyol A, Roura P, Bertran E (2005) Si_3N_4 single-crystal nanowires grown from silicon micro- and nano particles near the threshold of passive oxidation. Applied Physics Letters 87(19): 192114.

[11] Chen F, Li Y, Liu W, Shen Q, Zhang L M, Jiang Q, Lavernia E J, Schoenung J M (2009) Synthesis of α silicon nitride single-crystalline nanowires by nitriding cryomilled nanocrystalline silicon powder. Scripta Materialia 60(9):737-740.

[12] Kim H Y, Park J, Yang H (2003) Synthesis of silicon nitride nanowires directly from the silicon substrates. Chemical Physics Letters 372(1-2):269-274.

[13] Omidi Z, Bakhshi S R, Ghasemi A (2014) Evaluation of processing parameters effects on the formation of Si_3N_4 wires synthesized by means of ball milling and nitridation route. Advanced Powder Technology 25(6):1667-1671.

[14] Liu D, Shi T L, Zhang L, Xi S, Tang Z R, Li X P (2011) Bulk synthesis of long silicon nitride nanowires on silicon wafer. In: Nanotechnology Materials and Devices Conference (NMDC), 2011 IEEE; 18-21 October 2011; Jeju. p. 512-516.

[15] Zhang Y J, Wang N L, He R R, Liu J, Zhang X Z, Zhu J (2001) A simple method to synthesize Si_3N_4 and SiO_2 nanowires from Si or Si/SiO_2 mixture. Journal of Crystal Growth 233(4):803-808.

[16] Zheng C S, Yan Q Z, Xia M (2012) Combustion synthesis of SiC/Si_3N_4-NW composite powders: The influence of catalysts and gases. Ceramics International 38(6):4549-4554.

[17] Guo C L, Zheng X, Ma X J, Xu L Q, Qian Y T (2008) Solvothermal synthesis of Si_3N_4 nanomaterials at low temperature. Journal of the American Ceramic Society 91(5):1725-1728.

[18] Kenry, Lim C T (2013) Synthesis, optical properties, and chemical-biological sensing applications of one-dimensional inorganic semiconductor nanowires. Progress in Materials Science 58(5):705-748.

[19] Wang W Q, Zou X P, Zhou N J, Zhu G, Wang G Y, Peng Z S (2013) Synthesis of ultralong Si_3N_4 nanowires by a simple thermal evaporation method. Rare Metals 32(2):186-190.

[20] Shen G Z, Bando Y, Liu B D, Tang C C, Huang Q, Golberg D (2006) Systematic investigation of the

formation of [1]D α-Si_3N_4 nanostructures by using a thermal-decompositon/nitridation process. Chemistry - A European Journal 12(11):2987-2993.

[21] Tsu D V, Lucousky G (1986) Silicon nitride and silicon diimide grown by remote plasma enhanced chemical vapor deposition. Journal of Vacuum Science and Technology A4 4:480-485.

[22] Viera G, Andújar J L, Sharma S N, Bertran E (1998) Nanopowder of silicon nitride produced in radio frequency modulated glow discharges from SiH_4 and NH_3. Surface and Coatings Technology 100-101:55-58.

[23] Wang F, Jin G Q, Guo X Y (2006) Sol-gel synthesis of Si_3N_4 nanowires and nanotubes. Materials Letters 60:330-333.

[24] Huo K, Ma Y W, Hu Y M, Fu J J, Lu B, Lu Y N, Hu Z, Chen Y (2005) Synthesis of single-crystalline α-Si_3N_4 nanobelts by extended vapour-liquid-solid growth. Nanotechnology 16(10):2282-2287.

[25] Yang W Y, Wang H T, Liu S Z, Xie Z P, An L N (2007) Controlled Al-Doped single-crystalline silicon nitride nanowires synthesized via pyrolysis of polymer precursors. The Journal of Physical Chemistry B 111(16):4156-4160.

[26] Riley F L (2000) Silicon nitride and related materials. Journal of the American Ceramic Society 83(2): 245-265.

[27] Wang Q S, Cong R D, Li M, Zhang J, Cui Q L (2010) A simple method to synthesize α-Si_3N_4, β-SiC and SiO_2 nanowires by carbothermal route. Journal of Crystal Growth 312(14):2133-2136.

[28] Rao C N R, Deepak F L, Gundiah G, Govindaraj A (2003) Inorganic nanowires. Progress in Solid State Chemistry 31(1-2):5-147.

[29] Deshmukh S, Jen K P, Santhanam S (2012) Comparison of silicon nitride nanofibers synthesized using silica nanopowders and silica gel. Materials Sciences and Applications 3(8):523-529.